Guided Mode Expansion Analysis of Photonic Crystal Surface Emitting Lasers

Pawel Strzebonski*, Kent Choquette
Electrical and Computer Engineering Department
University of Illinois, Urbana, Illinois 61801 USA
*strzebo2@illinois.edu

Abstract

We use guided mode expansion (GME) to analyze surface etch photonic crystal (PhC) structures in order to evaluate photonic crystal surface emitting laser (PCSEL) designs and their optical modes. The three dimensional optical modeling reveals that the modal quality factor and modal coupling to the substrate vary periodically with increased PhC etch depth. We propose a method based on GME modeling to analyze the in-plane modes of finite-sized PCSEL lattices.

Index Terms

Photonic Crystal, Diode Laser, Photonic Crystal Surface Emitting Laser, Guided Mode Expansion

I. Nomenclature

A. Abbreviations

- PCSEL — photonic crystal surface emitting laser
- PhC — photonic crystal
- FDTD — finite-difference time-domain
- RCWA — rigorous coupled wave analysis
- PWE — plane-wave expansion
- GME — guided mode expansion
- DBR — distributed Bragg reflector
- VCSEL — vertical cavity surface emitting laser
- DFB — distributed feedback
- Q — quality (factor)

B. Symbols

- λ_0 — free-space wavelength

- Λ photonic crystal period
- m_B Bragg order
- $\overline{n}$ effective refractive index
- m_D diffraction order
- ω angular frequency (radians per second)
- τ_p cavity photon lifetime
- α_i internal loss coefficient
- α_m cavity mirror loss coefficient
- v_g group velocity
- Q quality factor

II. Introduction

Photonic crystal surface emitting lasers, commonly referred to as PCSELs, are a class of semiconductor diode lasers with in-plane propagation/oscillation of the optical mode that use photonic crystals (PhCs, structures with periodic variation of refractive index) to provide in-plane confinement and diffractive out-coupling to surface emissions. Recently PCSELs have gathered attention as a promising semiconductor diode laser structure that provide high spectral and spatial brightness in a manner that is scalable to higher powers. Orif. Susuma Noda has been the primary investigator of these structures, working on the earliest manifestation [1] as well as their newest and most advanced forms [2]. The PhC structure effectively controls the optical modes across a broad gain area, providing a stabilized lasing wavelength and narrower lasing spectrum bandwidth, as well as distributed diffractive emission from a broad area that gives a high quality and low divergence beam. Reported power metrics have been constantly increasing along with device area:

- 2014, 200 μm diameter, 1.5 Watts continuous or 3.4 Watts pulsed, M^2=1 up to 0.5 Watts [3]
- 2018, 500 μm diameter, 10 Watts pulsed with M^2<2.5 [4]
- 2021, 3 mm diameter, 150 Watts pulsed [2]

It is expected that further scaling in size and power to kilowatt levels is possible [2].

The specifics of PCSEL designs can vary greatly. Generally, an epitaxially grown gain region is embedded within a dielectric slab waveguide providing optical confinement in the epitaxial dimension, and a PhC structure is located in proximity to the optical mode to provide optical feedback/confinement within the wafer plane. Various PhC designs have been used. The PhCs have include triangular lattices [1], square lattices [5], and centered-rectangular lattices [6]. The PhC etch patterns have included circles [1], ellipses [7], equilateral triangles [8], right isosceles triangles [3], and others. Past PCSELs have used PhCs that were high index-contrast air/semiconductor structures embedded within the laser structure [1] or etched into the surface [9], while others have used low index-contrast semiconductor/semiconductor structures [10].

With all the numerous design parameters that greatly modify the laser mode and beam properties, the ability to effectively model potential PCSEL structures and evaluate them becomes a critical component of the design and engineering process. Various modeling methods have been proposed and applied to PCSELs in the past. This includes methods such as finite-difference time-domain (FDTD) simulation [11], rigorous coupled wave analysis (RCWA) [12], modal index analysis [13], coupled-wave theory [14], and plane-wave expansion (PWE) [15]. These methods are varied in the ability to effectively model a PCSEL structure as well as the results that they produce for subsequent analysis.

This work applies a different electromagnetic modeling method to the problem of evaluating PCSEL structures, namely guided mode expansion (GME) [16]. We will analyze a theoretical structure that uses a surface etched square lattice of right isosceles triangles. However, GME is not limited in applicability to only these sorts of structures. The PhC structure has been demonstrated to reach Watt-levels of power [3] and surface etch structures represent a relatively simple fabrication process (as compared to embedded PhC designs that generally require either regrowth [17, 10] or wafer fusion [1]).

First the Bragg condition and diffraction of the photonic crystal is discussed. The quality factor is introduced for loss induced in-plane and by the photonic crystal. Next GME is applied to analyze an InP PCSEL emitting at 1550 nm. The effects of etch depth and higher order resonances are explored.

III. Theory and Methods

A. Bragg Resonance and Diffraction in Photonic Crystals

Photonic crystals are a class of structures with periodic refractive index structuring that produce distributed resonant effects at (in-material) wavelengths commensurate with the period of the PhC. One dimensional forms of PhCs include distributed Bragg reflectors (DBRs) used in vertical cavity surface emitting lasers (VCSELs) and the gratings in distributed feedback (DFB) lasers. Two dimensional forms of PhCs have been used in edge-emitting lasers for mode control, as a confinement means for nanolasers, and form the basis for most PCSELs.

The period (Λ) of a PhC is often related to the in-material wavelength of the Bragg wavelength (free-space wavelength λ_0) via the effective index within the PhC ($\overline{n}$):

$$\Lambda = \frac{m_B \lambda_0}{2\overline{n}} \tag{1}$$

The m_B term is the positive integer Bragg order. Using higher order Bragg resonances ($m_B > 1$) gives larger PhC periods that are some multiple of the in-material half-wavelength (which may be desirable from an ease of fabrication perspective), however higher order PhCs tend to be associated with lesser mode control and higher losses (as will be discussed later).

Equation (1) is generally acceptable for one dimensional PhC structures with an oscillation along the direction of periodicity, but for two dimensional PhC structures, such as those

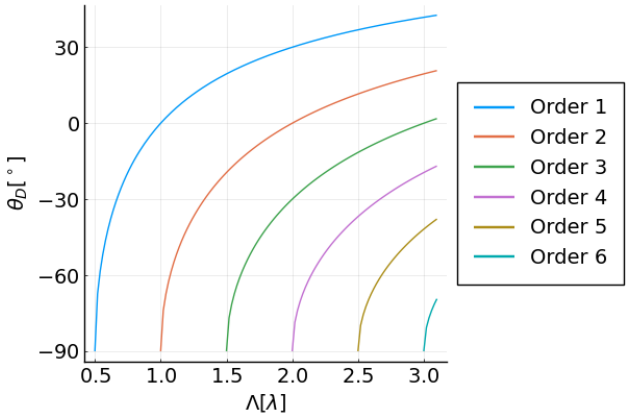

Fig. 1: Diffraction angle as a function of diffraction order and grating period (in multiples of the in-material wavelength).

commonly used in PCSELs, this fails to incorporate all of the higher order resonances. Consider a two-dimensional square lattice PhC with two axes (x and y) of equal period. A optical wave propagating in the $\hat{x}$ or $\hat{y}$ direction would see a periodic index structure repeating at the lattice period Λ, but a wave propagating in another direction would also see period index structuring with a different effective period. To incorporate these non-axis-aligned higher order resonances we define a new equation for the PhC period that uses two Bragg order terms, $m_{B,x}$ and $m_{B,y}$, that correspond to the effective Bragg order along each of the axes (and in this case one of the two Bragg order terms may be zero):

$$\Lambda = \frac{\sqrt{m_{B,x}^2 + m_{B,y}^2}\lambda_0}{2\overline{n}} \tag{2}$$

Note that Equation (2) is only valid for a two-dimensional square lattice.

The Bragg resonance effect provides the in-plane optical feedback and confinement that provides the mode control in PCSELs, but diffraction provides the critical out-coupling to create what would otherwise be an edge-emitting laser into a surface emitting laser. Diffraction is also a resonant effect that relies on periodic structuring. Diffraction of order m_D (non-negative integer) will out-couple light at an angle θ_D from the surface-normal [18]:

$$\theta_D = \sin^{-1}\left(\overline{n} - m_D\frac{\lambda_0}{\Lambda}\right) \tag{3}$$

We calculate the valid diffraction angles as a function of the grating period using Equation (3) and plot the results in Fig. 1. As we want diffractive out-coupling to surface-normal emission ($\theta_D = 0$), we find that our PhC would need a period that is an integral multiple of the in-material wavelength. Our observation from Fig. 1 implies that we may have both the in-plane feedback and out-of-plane out-coupling that PCSELs need under the condition that $m_B = 2m_D$. While these results suggest that we may be able to use higher-order Bragg resonances and diffraction in PCSEL design, the effectiveness of such a design remains to be seen. As Fig. 1 shows, higher PhC periods tend to have more solutions for potential

diffractive out-coupling via the various diffraction orders, so while surface-normal emission is possible, it may be less efficient than emission into the other orders at non-surface-normal angles.

B. Photonic Crystal Modes, Infinite and Finite

Analysis of photonic crystals often invokes the photonic band diagram, that plots the frequency of the optical field solutions within a infinite PhC as a function of the in-plane wave-vector [19]. PCSELs operate at what is generally referred to as the Γ-point of the PhC band diagram [1], where the wave-vector is proportional to an integral multiple of the PhC period. In an infinite PhC lattice the solutions for the modes form continuous bands (except for the discontinuities at the photonic band-edge/band-gap). The group velocity is related to the slope of the photonic bands [19], and at the edges of the bands (such as near the Γ-point of PCSEL band diagrams) the slope approaches zero, indicating a "slow light" effect.

However, practical PCSEL structure do not have infinite PhC lattices. These finite-extent structures have constraints imposed on the wave-vectors based on the cavity that the finite PhC lattice creates [19], such that when translated to the band diagram, manifests itself as discrete points on the diagram. If we have a finite PhC with N-many periods, then we can estimate the permitted wave-vector magnitude values k_m to be:

$$k_m \approx \frac{m\pi}{N\Lambda} \tag{4}$$

For integer values of the finite in-plane mode index m. We can see in Equation (4) that as the lattice grows larger (that is, N is larger) then the spacing between the permitted modal wave-vectors will decrease due to the N term in the denominator, as expected.

C. Quality Factor and Group Velocity

In our analysis of PhCs for PCSELs, we will quantify the interaction between the optical mode and PhC in part using the quality, or Q, factor. Quality factors are used in various engineering contexts and have numerous definitions. It can be defined in terms of the complex resonance wavelength ω that some simulations return [12]:

$$Q = -\frac{\Re(\omega)}{2\Im(\omega)} \tag{5}$$

In optical cavities it can be related to the photon lifetime τ_p or group velocity v_g and mirror/internal loss coefficients α_m and α_i [20]:

$$Q = \omega\tau_p = \frac{\omega}{v_g(\langle\alpha_i\rangle + \alpha_m)} \tag{6}$$

Or more generally it is defined in terms of energy and power [18]:

$$Q = 2\pi \frac{\text{Energy stored}}{\text{Energy dissipated per optical cycle}} \tag{7}$$

Q values can be used in several ways to elucidate the behavior of PhC structures. Higher Q is generally associated with lower losses from a cavity, likely implying lower threshold gain for an optical mode. Differences in Q between modes can relate differences in modal losses and modal threshold gains, potentially allowing us to predict modal discrimination and selection within a cavity.

We can identify two main forms of optical loss in our (idealized) PCSEL structures. First is loss due to PhC diffractive out-coupling through the surface that occurs in an infinite PhC lattice. The GME software will return a Q factor that quantifies these losses. The second form of optical loss we consider is loss from the optical mode leaking through the edges of a finite PhC lattice. These losses are not calculated directly by GME software we use. However, we can quantify an estimate if we model the finite PCSEL structure as an optical cavity with in-plane oscillation. We can estimate the mirror loss for the optical cavity model and incorporate the PhC effects via the group velocity term in Equation (6) (the group velocity can be derived from the PhC mode bands that GME software can solve for). Once we have calculated the PhC diffractive losses and lateral losses as Q factors, we can combine the two to obtain a single overall modal Q factor:

$$Q_{\text{mode}} = \frac{1}{\frac{1}{Q_{\text{PhC}}} + \frac{1}{Q_{\text{lateral}}}} \tag{8}$$

D. Guided Mode Expansion

As previously mentioned, various methods have been previously used to model and analyze PCSEL structures. They have varied greatly in their capabilities, runtime performance, and ease of analysis of the simulation results. There are a couple capabilities that guided our choice of modeling method/software:

- Solve for PhC resonant mode frequencies (in order to align resonance to gain)
- Solve for PhC resonant mode fields (in order to analyze near-field/far-field/beam)
- Solve for PhC resonant mode Q (in order to quantify diffractive losses)
- Solve for PhC band diagram (in order to calculate group velocity and estimate edge losses)
- Capable of modeling three dimensional structure (simultaneous modeling of PhC and epitaxial structure)

FDTD is a very capable method that can be applied to all sorts of electromagnetic problems, including PCSELs [11]. It has all of the desired capabilities, but it can be computationally intensive and the time-domain nature can make analyzing the results relatively complicated relative to frequency-domain algorithms for our application. PWE is a common and intuitive choice for PhC modeling [15], but it is not well suited for analyzing finite-extent, non-periodic dimensions (such as the epitaxial structure), limiting it's usefulness for our analysis. RCWA is capable of modeling the full three dimensional structure and calculating the Q factor and resonance frequencies, but analyzing the fields and obtaining the PhC band diagram is somewhat involved [12]. GME, on the other hand, provides all of the capabilities we desire in a relatively straightforward manner [16].

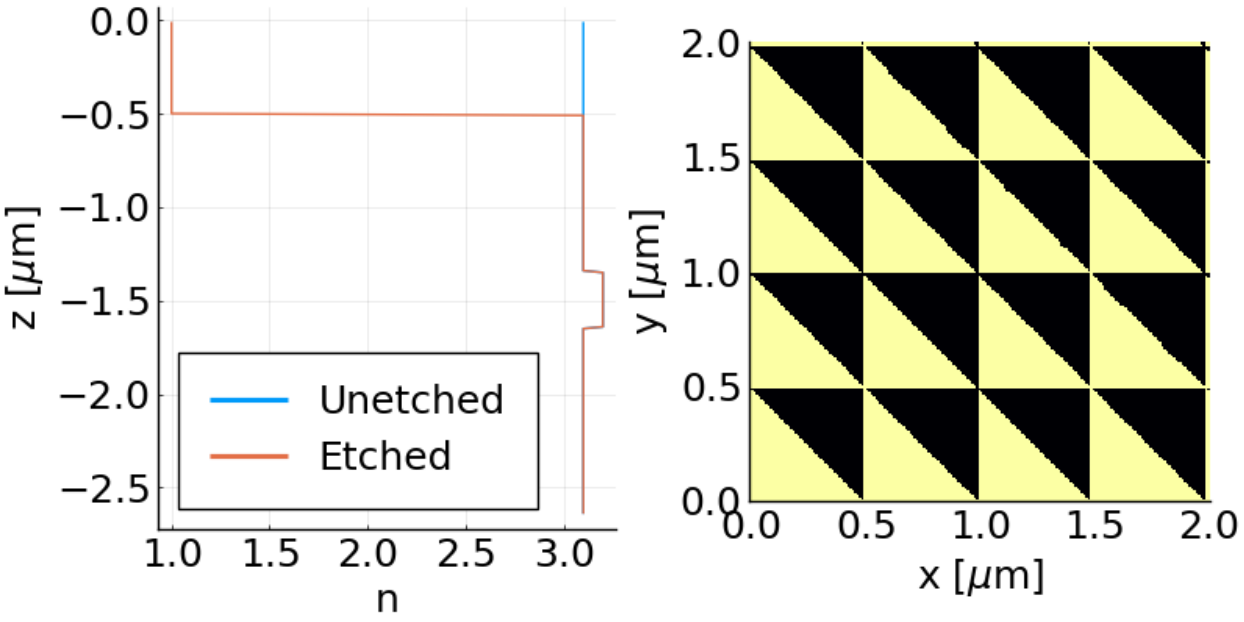

(a) Epitaxial cross-section

(b) PhC cross-section

Fig. 2: Cross-sections of a hypothetical surface-etch PCSEL.

In our analysis, we will use the free and open source GME software legume [21]. This software exposes GME functionality via a programmatic Python language interface. The general modeling process is as follows:

1) Define the PhC lattice (lattice period and lattice basis vectors)
2) Define top and bottom interface relative permittivity values (air and semiconductor substrate)
3) Define the thickness and relative permittivity of each epitaxial layer (with any etched PhC features in the layer, if relevant)
4) Define the wave-vectors to solve for (for PCSELs, these should be at the Γ point or in it's vicinity) and which modes to solve for (depends on the lattice type and the design resonance order)
5) Run GME simulation
6) Obtain solutions for the modal frequency, PhC Q factor, fields, and coupling coefficients to the top/bottom interfaces and analyze them

In our analysis, we will consider a hypothetical surface etch PCSEL that would approximate a structure in the InP/InGaAs material system targeting a wavelength of 1550 nm. We assume a waveguide core layer of 300 nm thickness and refractive index 3.2 with a cladding of refractive index 3.1 (1300 nm of upper cladding between the core and upper air surface). In Fig. 2 we illustrate such a structure with a right isosceles triangles etched on a rectangular lattice of 496 nm period that has been etched 500 nm through the surface.

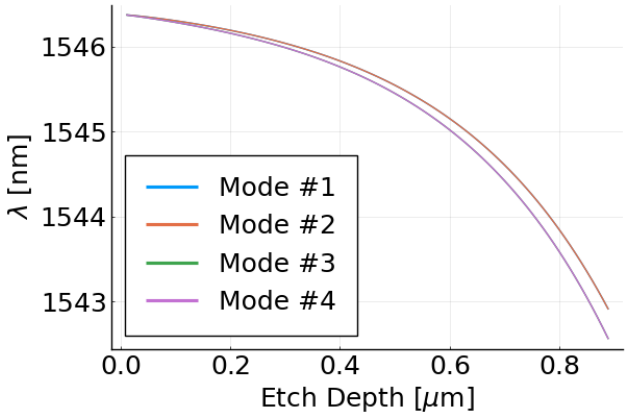

Fig. 3: Free-space wavelengths of the PhC resonant modes in a first-order PCSEL.

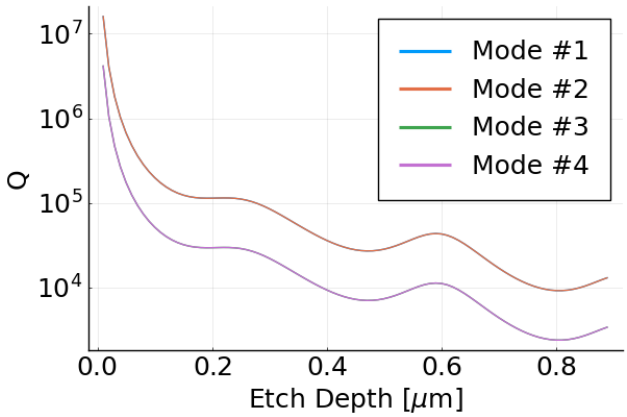

Fig. 4: PhC quality factor of the PhC resonant modes in a first-order PCSEL.

IV. Results

A. Modeling Effects of Etch Depth

First, we explore the effects of PhC surface etch depth on the first-order resonances. For the first-order structure we use a PhC lattice period of 496 nm, and we solve for the four modes that have a resonance wavelength near the desired 1550 nm.

In Fig. 3 we plot the free-space wavelength for the four PhC modes as a function of etch depth. While there are four modes, we can only discern two lines in Fig. 3 as we have two pairs of nearly degenerate modes. We find that as we etch deeper the resonances shift towards shorter wavelengths. This is consistent with published experimental observation [9]. We also observe that the wavelength splitting between the two pairs of modes increases with increased etch depth.

In Fig. 4 we can see the quality factors incorporating the PhC diffraction loss. We find that one pair of modes has a higher Q factor than the other, and that all modes have a

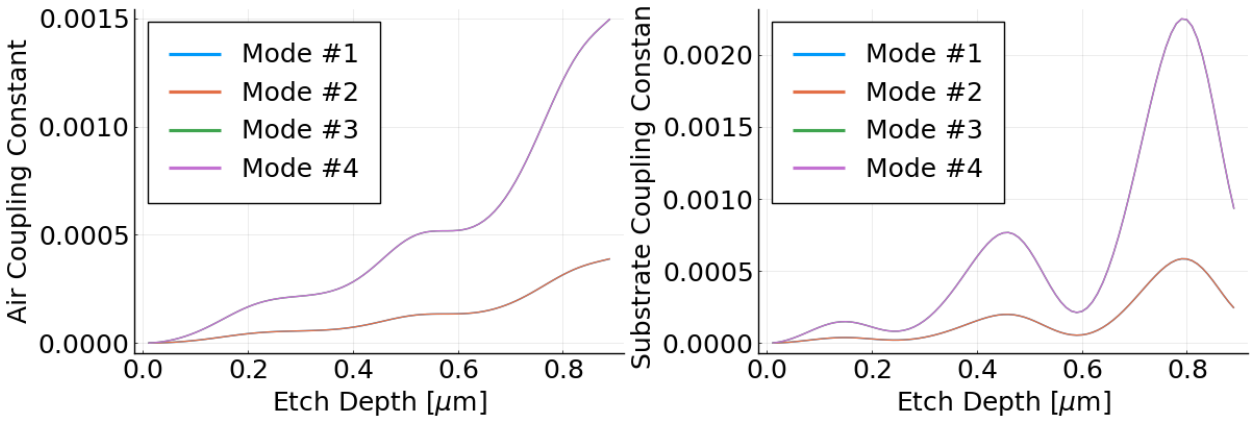

(a) Coupling coefficient to air

(b) Coupling coefficient to substrate

Fig. 5: Coupling coefficients of the PhC resonant modes in a first-order PCSEL.

general trend of decreasing Q with increased etch depth. This is expected as etching deeper brings the PhC closer to the mode within the epitaxially defined waveguide, increasing the interaction between the mode and the PhC and increasing the diffraction losses (lowering Q). Less expected is the periodic variation in Q as a function of etch depth. To try to investigate why, we look at the coupling coefficients for the modes.

Fig. 5 shows the modal coupling coefficients to the air and substrate. Higher coupling coefficient values reflect higher radiation losses. These modeling results show a general trend of increase losses to air with increased etch depth, but the losses to the substrate show a general increasing trend with very strong periodic etch-dependent variation. Comparing the coupling coefficients to air and substrate we find that the coupling to substrate alternates between being higher and lower than coupling the the air. This implies that controlling the etch depth may be a way of biasing emissions into the desired direction (top vs bottom emission).

B. Modeling Higher-Order Resonance

We can explore higher order resonances by modeling structures with appropriately larger lattice periods and evaluating the corresponding higher order resonant modes. In our case, the next set of resonances is the set of the next four modes in a PCSEL with the same right isosceles triangle but now with a 705 nm period.

In Fig. 6 we plot the free-space wavelength for the four PhC modes as a function of etch depth. As before, the resonance wavelength shows a decreasing trend with increased etch depth, and now the degeneracy between the modes is broken as we can make out four distinct curves.

Fig. 7 plots the corresponding modal PhC Q as a function of etch depth. As before, there is a decreasing trend with increased etch depth. The periodic variation that was observed

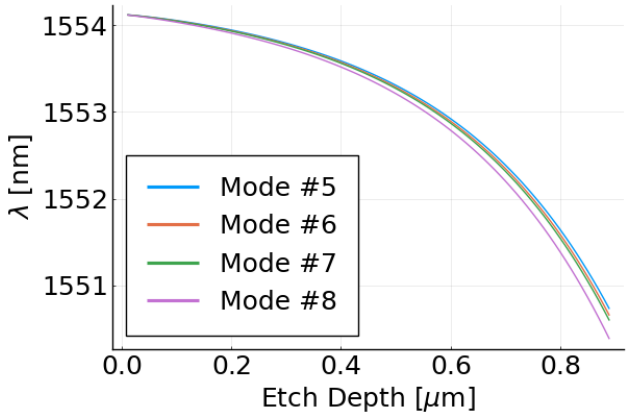

Fig. 6: Free-space wavelengths of the PhC resonant modes in a higher-order PCSEL.

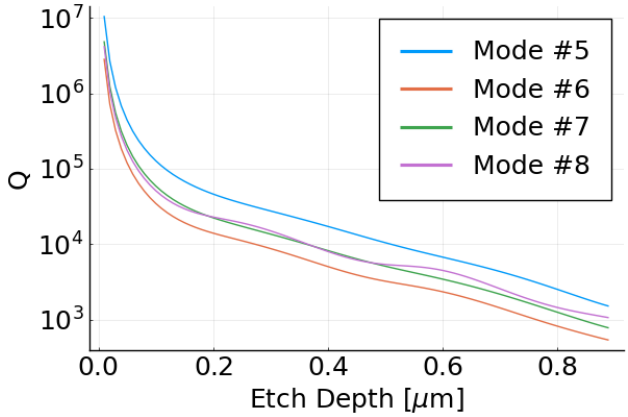

Fig. 7: PhC quality factor of the PhC resonant modes in a higher-order PCSEL.

in the first-order modes either does not occur or is much less pronounced.

Fig. 8 shows that there is still significant variation in the coupling to the substrate. Interestingly, we find that at an etch depth around 650 nm the coupling to the substrate appears to be relatively negligible compared to the coupling to air, implying that biasing vertical emissions toward top emission as opposed to bottom emission may be possible in these lasers.

C. Modeling Finite Photonic Crystal In-Plane Modes

One of the challenges in scaling PCSELs to greater areas involves controlling the balance between the in-plane feedback and out-of-plane diffractive emission in a manner that will support broad area single mode lasing. We attempt to model finite PCSEL size dependent modal behavior by using GME to solve at wave-vectors around the Γ-point. Once again we return to the first-order structure with a lattice period of 496 nm, but now we fix the etch depth and just look at the different photonic mode bands.

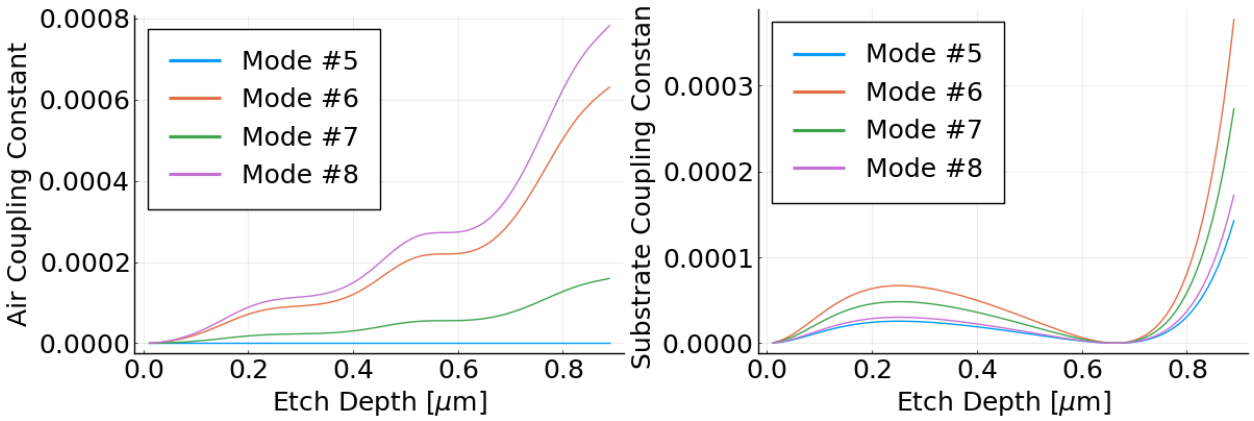

(a) Coupling coefficient to air

(b) Coupling coefficient to substrate

Fig. 8: Coupling coefficients of the PhC resonant modes in a higher-order PCSEL.

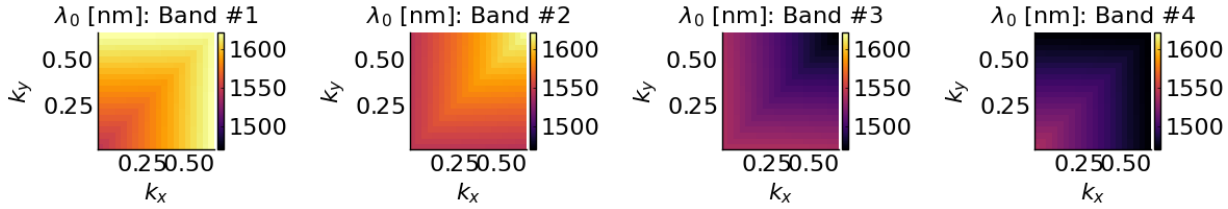

Fig. 9: Free-space wavelengths of the PhC resonant modes in a first-order PCSEL.

In Fig. 9 we plot the free-space wavelength for the four PhC bands of the first-order resonances. The Γ-point is at the lower left corners of the figures where $k_x = k_y = 0$. As this structure was designed for 1550 nm resonance at the Γ-point, it is not surprising that the higher-order in-plane modes shift away from the design wavelength.

Fig. 10 illustrates the Q factor for the diffractive losses for the in-plane modes. The different bands show varied trends in Q, as some of them have higher Q along the diagonal,

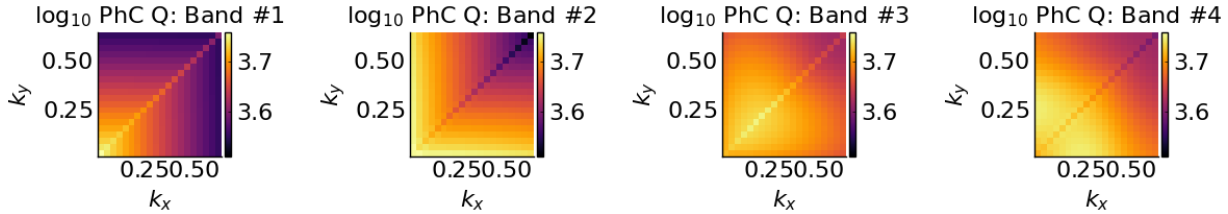

Fig. 10: PhC quality factor of the PhC resonant modes in a first-order PCSEL.

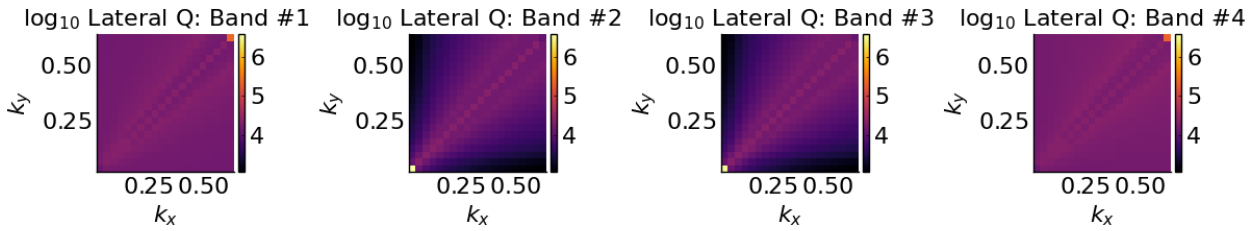

Fig. 11: Estimated in-plane quality factor of the PhC resonant modes in a first-order PCSEL.

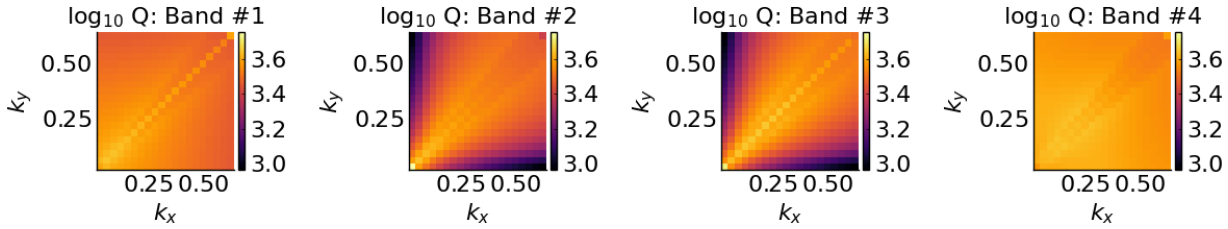

Fig. 12: Estimated overall quality factor of the PhC resonant modes in a first-order PCSEL.

others away from the diagonal, some have lower Q the closer to the Γ-point, while others higher Q.

The previous figures involved quantities directly calculated using GME software. In order to deduce the in-plane losses for the lateral Q factor we treat the finite in-plane lattice as an optical cavity (with some mirror loss coefficient) with an effective group velocity derived from the band diagram (Fig. 9) for each in-plane mode, in accordance to Equation (6). We calculate the quality factor for the in-plane loss in Fig. 11 assuming a square lattice of certain size. As with the PhC diffraction Q factor, the different bands and modes show varied trends. These results show that overall the estimated Q factors for in-plane losses are much higher than for the PhC Q factor, indicating that our model would estimate most of the optical loss to be to the surface-normal emissions as opposed to loss through the lattice edges. However, were a different lattice size chosen the edge losses could just as well been higher than PhC diffraction losses.

In order to analyze modal selection and discrimination in finite-size PhC lattices, we want to calculate the overall quality factor for each of the in-plane PhC modes. We combine the GME calculated PhC Q with the estimated lateral Q to get an estimate for the overall finite cavity Q, illustrated in Fig. 12. As in our hypothetical example the PhC Q was lower than the lateral Q, we find that the overall Q is primarily determined by the lower of the two (PhC Q).

V. Conclusion

We have used guided mode expansion to analyze an example square-lattice photonic crystal with right isosceles triangle features to model surface etch photonic crystal surface emitting lasers. We have found that increasing the etch depth shifts resonance wavelengths toward shorter wavelength, consistent with published experimental results. The model indicates a general trend of decreased quality factor with increased etch depth with some periodic variation due to periodic variation in the coupling to the substrate. This periodic variation may allow for engineering a bias towards either top or bottom emissions via control of the surface etch depth. GME analysis of photonic crystals with larger periods indicates higher-order resonances can be found at the desired wavelength, hinting at the possibility of higher-order resonance PCSELs that have larger feature sizes and lower lithography requirements. Finally, we have proposed a method of combining GME analysis with optical cavity modeling to estimate the quality factor of in-plane PhC modes in finite sized PCSELs, that may enable evaluating size-dependent modal behavior of PCSELs, however the model has not yet been verified using experimental results.

References

[1] Masahiro Imada, Susumu Noda, Alongkarn Chutinan, Takashi Tokuda, Michio Murata, and Goro Sasaki. Coherent two-dimensional lasing action in surface-emitting laser with triangular-lattice photonic crystal structure. Applied Physics Letters, 75(3):316–318, July 1999. doi: 10.1063/1.124361. URL https://doi.org/10.1063/1.124361.

[2] Susumu Noda. Progress of photonic crystal surface-emitting lasers: Paradigm shift for LiDAR sensing and laser processing. In Andrea M. Armani, Alexis V. Kudryashov, Alan H. Paxton, Vladimir S. Ilchenko, and Julia V. Sheldakova, editors, Laser Resonators, Microresonators, and Beam Control XXIII. SPIE, March 2021. doi: 10.1117/12.2593114. URL https://doi.org/10.1117/12.2593114.

[3] Kazuyoshi Hirose, Yoshitaka Kurosaka, Akiyoshi Watanabe, Takahiro Sugiyama, Yong Liang, and Susumu Noda. Demonstration of watt-class high-power photonic-crystal lasers. In CLEO: 2014. OSA, 2014. doi: 10.1364/cleo_si.2014.sw3g.3. URL https://doi.org/10.1364/cleo_si.2014.sw3g.3.

[4] Masahiro Yoshida, Menaka De Zoysa, Kenji Ishizaki, Yoshinori Tanaka, Ranko Hatsuda, Masato Kawasaki, Bong-Shik Song, and Susumu Noda. 10 w high-power and high-beam-quality pulsed operation of double-hole photonic-crystal surface-emitting lasers. In Conference on Lasers and Electro-Optics. OSA, 2018. doi: 10.1364/cleo_si.2018.sf1g.3. URL https://doi.org/10.1364/cleo_si.2018.sf1g.3.

[5] M. Yckoyama, M. Imada, A. Chutinan, and S. Noda. Fabrication of surface-emitting laser with two-dimensional square-lattice photonic crystal. In Technical Digest. CLEO/Pacific Rim 2001. 4th Pacific Rim Conference on Lasers and Electro-Optics (Cat. No.01TH8557). IEEE. doi: 10.1109/cleopr.2001.967709. URL https://doi.org/10.1109/cleopr.2001.967709.

[6] Seita Iwahashi, Kyosuke Sakai, Yoshitaka Kurosaka, Yong Liang, Wataru Kunishi, Dai Ohnishi, and Susumu Noda. Two-dimensional photonic-crystal lasers with centered-rectangular lattice structure. In 2009 IEEE LEOS Annual Meeting Conference

Proceedings. IEEE, October 2009. doi: 10.1109/leos.2009.5343177. URL https://doi.org/10.1109/leos.2009.5343177.

[7] S. Noda. Polarization mode control of two-dimensional photonic crystal laser by unit cell structure design. Science, 293(5532):1123–1125, August 2001. doi: 10.1126/science.1061738. URL https://doi.org/10.1126/science.1061738.

[8] Wataru Kunishi, Dai Ohnishi, Eiji Miyai, Kyosuke Sakai, and Susumu Noda. High-power single-lobed surface-emitting photonic-crystal laser. In 2006 Conference on Lasers and Electro-Optics and 2006 Quantum Electronics and Laser Science Conference. IEEE, 2006. doi: 10.1109/cleo.2006.4627795. URL https://doi.org/10.1109/cleo.2006.4627795.

[9] Zong-Lin Li, Shen-Chieh Lin, Gray Lin, Hui-Wen Cheng, Kien-Wen Sun, and Chien-Ping Lee. Effect of etching depth on threshold characteristics of GaSb-based middle infrared photonic-crystal surface-emitting lasers. Micromachines, 10(3):188, March 2019. doi: 10.3390/mi10030188. URL https://doi.org/10.3390/mi10030188.

[10] Zijun Bian, Katherine J. Rae, Adam F. McKenzie, Ben C. King, Nasser Babazadeh, Guangrui Li, Jonathan R. Orchard, Neil D. Gerrard, Stephen Thoms, Donald A. MacLaren, Richard J. E. Taylor, David Childs, and Richard A. Hogg. 1.5 μm epitaxially regrown photonic crystal surface emitting laser diode. IEEE Photonics Technology Letters, 32(24):1531–1534, December 2020. doi: 10.1109/lpt.2020.3039059. URL https://doi.org/10.1109/lpt.2020.3039059.

[11] Mitsuru Yokoyama and Susumu Noda. Finite-difference time-domain simulation of two-dimensional photonic crystal surface-emitting laser. Optics Express, 13(8):2869, 2005. doi: 10.1364/opex.13.002869. URL https://doi.org/10.1364/opex.13.002869.

[12] Alex Y. Song, Akhil Raj Kumar Kalapala, Weidong Zhou, and Shanhui Fan. First-principles simulation of photonic crystal surface-emitting lasers using rigorous coupled wave analysis. Applied Physics Letters, 113(4):041106, July 2018. doi: 10.1063/1.5045486. URL https://doi.org/10.1063/1.5045486.

[13] Guangrui Li, Jayanta Sarma, Iain Butler, Richard J. E. Taylor, David T. D. Childs, and Richard A. Hogg. Modelling and device simulation of photonic crystal surface emitting lasers based on modal index analysis. In 2018 IEEE International Semiconductor Laser Conference (ISLC). IEEE, September 2018. doi: 10.1109/islc.2018.8516220. URL https://doi.org/10.1109/islc.2018.8516220.

[14] K. Sakai, E. Miyai, and S. Noda. Coupled-wave theory for square-lattice photonic crystal lasers with TE polarization. IEEE Journal of Quantum Electronics, 46(5):788–795, May 2010. doi: 10.1109/jqe.2009.2037597. URL https://doi.org/10.1109/jqe.2009.2037597.

[15] Richard J E Taylor, David M Williams, Jon R Orchard, David T D Childs, Salam Khamas, and Richard A Hogg. Band structure and waveguide modelling of epitaxially regrown photonic crystal surface-emitting lasers. Journal of Physics D: Applied Physics, 46(26):264005, June 2013. doi: 10.1088/0022-3727/46/26/264005. URL https://doi.org/10.1088/0022-3727/46/26/264005.

[16] Lucio Claudio Andreani and Dario Gerace. Photonic-crystal slabs with a triangular lattice of triangular holes investigated using a guided-mode expansion method. Physical Review B, 73(23), June 2006. doi: 10.1103/physrevb.73.235114. URL https://doi.org/10.1103/physrevb.73.235114.

[17] M. De Zoysa, M. Yoshida, M. Kawasaki, K. Ishizaki, R. Hatsuda, Y. Tanaka, and S. Noda. Photonic crystal lasers fabricated by MOVPE based on organic arsenic

source. IEEE Photonics Technology Letters, 29(20):1739–1742, October 2017. doi: 10.1109/lpt.2017.2748980. URL https://doi.org/10.1109/lpt.2017.2748980.

[18] Lukas Chrostowski and Michael Hochberg. Silicon Photonics Design. Cambridge University Press, 2015. doi: 10.1017/cbo9781316084168. URL https://doi.org/10.1017/cbo9781316084168.

[19] John D. Joannopoulos, Steven G. Johnson, Joshua N. Winn, and Robert D. Meade. Photonic Crystals. Princeton University Press, October 2011. doi: 10.2307/j.ctvcm4gz9. URL https://doi.org/10.2307/j.ctvcm4gz9.

[20] Larry A. Coldren, Scott W. Corzine, and Milan L. Mašanović. Diode Lasers and Photonic Integrated Circuits. John Wiley & Sons, Inc., Mar 2012. doi: 10.1002/9781118148167. URL https://doi.org/10.1002/9781118148167.

[21] Momchil Minkov, Ian A. D. Williamson, Lucio C. Andreani, Dario Gerace, Beicheng Lou, Alex Y. Song, Tyler W. Hughes, and Shanhui Fan. Inverse design of photonic crystals through automatic differentiation. ACS Photonics, 7(7):1729–1741, June 2020. doi: 10.1021/acsphotonics.0c00327. URL https://doi.org/10.1021/acsphotonics.0c00327.